CORRELATION BETWEEN MICROSTRUCTURE AND MECHANICAL PROPERTIES OF Al-Si CAST ALLOYS

F. Grosselle, G. Timelli, F. Bonollo, A. Tiziani, E. Della Corte

The influence of microstructure and process history on mechanical behaviour of cast Al-Si alloys is reported. In the present work, the EN-AC 46000 and 46100 aluminium alloys have been gravity cast using a step-bar permanent mould, with a range of thickness going from 5 to 20 mm. Metallographic and image analysis techniques have been used to quantitatively examine the microstructural parameters of the α-Al phase and eutectic Silicon. Microstructure has been also correlated with the results coming from the numerical simulation of the casting process. The results show that SDAS and length of eutectic silicon particles increase with section thickness, and consequently mechanical properties decrease.

KEYWORDS: aluminium alloys; EN-AC 46000; EN-AC 46100; SDAS; eutectic Si; microstructure; numerical simulation; permanent mould casting

INTRODUCTION

Mechanical properties of Al-Si cast alloys depend on several microstructural parameters. Grain size, secondary dendrite arm spacing (SDAS), distribution of phases, the presence of secondary phases or intermetallic compounds, the morphology of silicon particles (size, shape and distribution) and, finally, defects play a key role in the determination of the elastic and plastic behaviour of aluminium alloys [1-3].
In general, castings having a finer microstructure (quantitatively described by low SDAS values), induced by high solidification rate, show better mechanical properties. Many correlations between mechanical behaviour (UTS, YS, elongation) and SDAS can be found in literature [3-4]. It is worth mentioning that, on industrial production, the control of solidification rate (and therefore the SDAS values) is quite difficult to achieve [5], as consequence of the geometrical complexity and of the different wall thickness in the real-shaped casting. For this reason, reference castings are frequently employed when the solidification rate has to be accurately controlled and different microstructures have to be achieved. Therefore, in these castings, the solidification conditions can be set up by varying the thickness and the material of the mould, as well as the sample size [3,6]. In this way, the factors affecting SDAS, the relationship between SDAS and mechanical properties of cast aluminium alloys can be easily better assessed and these information can be subsequently transferred to real-shaped casting.
On the other hand, it is well known that SDAS is not the only factor affecting the mechanical behaviour of an alloy. For instance, the deformation behaviour of cast aluminium alloys is also affected by eutectic Si particles and intermetallic compounds which determine the initiation and the evolution of fracture [7-8]. In particular, for defect free castings, tensile fracture is initiated by cleavage of either brittle intermetallic particles or eutectic Si particles. The cleavage cracks are mainly perpendicular to the macroscopic principal strain, regardless of the particle orientation. Platelet particles with their length perpendicular to the tensile direction break because of cleavage along their length [9-10]. Therefore, it is easy to hypothesize that the fracture mechanism depends on the size and shape of Si or Fe-rich brittle phases. In detail, large and acicular particles are deleterious for mechanical properties reducing elongation to fracture and ultimate tensile strength [9].
In un-modified Al–Si cast alloys, the eutectic Si particles have a coarse, acicular and polyhedral morphology and the final mechanical properties of an alloy is characterized by their distribution in the microstructure. It was established that the size distribution of eutectic Si particles follows the lognormal distribution [8]. The probability density function of the three-parameters lognormal distribution can be written as:

$$(1) \quad f(d) = \frac{1}{(d-\tau)\sigma\sqrt{2\pi}} \exp\left[\frac{-(\ln(d-\tau)-\mu)^2}{2\sigma^2}\right]$$

where d is the diameter of Si particles, τ the threshold, σ the shape and μ is the scale parameter.

Fabio Grosselle, Giulio Timelli, Franco Bonollo, Alberto Tiziani
Dipartimento di Tecnica e Gestione dei Sistemi Industriali DTG, Università di Padova, Stradella S. Nicola, 3 I-36100 Vicenza, Italia (Email: grosselle@gest.unipd.it; Tel. 00 39 0444 99 87 54; Fax No. 00 39 0444 99 88 89)
Emilia Della Corte
Enginsoft Spa, via Giambellino 7, I-35129 Padova, Italia (Email: e.dellacorte@enginsoft.it; Tel. 00 39 049 77 05 311)

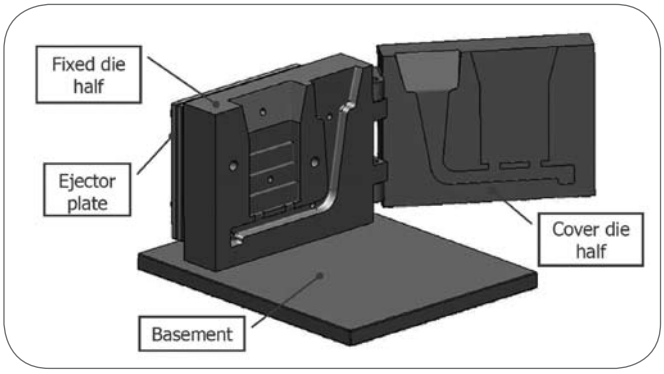

Fig. 1 ***Permanent mould die used in the present work.***
Stampo permanente in acciaio utilizzato in questo studio.

The aim of this work is to investigate the evolution of the microstructure (quantitatively evaluated by means of SDAS and Si-related parameters) as a function of the solidification time and to correlate microstructural parameters with the mechanical properties of a stepwise reference casting. The experiments considered cast thickness ranging from 5 to 20 mm.

EXPERIMENTAL PROCEDURE

Materials and experimental methods

The geometry of the die is shown in Fig. 1. The two part die is split along a vertical joint line passing through the pouring basin. To facilitate assembly and mutual location the die halves are hinged. The dimension of the whole die was 310x250x115 mm^3 and the thickness of the two die halves was 45 and 75 mm respectively. The die was made by an AISI H11 tool steel and the weight was around 140 kg. The casting, with the front and side views, is shown in Fig. 2. The step casting presented a range of thickness going from 5 to 20 mm and it was gated from the side of the thinnest step, while the riser, over the casting, ensured a good feeding. This configuration allows to obtain a range of solidification rates and consequently different microstructures in the casting. The weight of the aluminium alloy casting was 1.4 or 1 kg, including or not the runner system.

The step castings were produced with EN-AC 46000 and EN-AC 46100 alloys, two hypoeutectic aluminium–silicon alloys, in the form of ingots, whose composition is indicated in Tab. 1. The material was melted in an electric-induction furnace setup at 720±5°C. Before pouring, the melt was degassed with an argon-sulphur hexafluoride mixture (Ar/SF6 0.2%).

A semi-permanent layer of DYCOTE® F34 coating was spray applied on the die walls at the temperature of about 200°C according to standard practice [11].

Before pouring the melt, the temperature of the die was increased to about 250±10°C. Trough the use of thermocouples, the temperatures in different zones of the die were measured in order to evaluate the local temperature and assure a good reproducibility of the tests. The temperature in the die was in the range of (450–520)±3°C.

The castings were then sectioned and samples were drawn from each step. Radiographic inspection was carried out on tensile specimens before mechanical testing, in order to detect the presence of macrodefects.

Flat tensile test bars with rectangular cross section were obtained from the step castings (Fig. 3), in the middle and external zones of the castings. In this way it was possible to study the effect of the local temperature and the heat transfer on the solidification rate and, thus, on the microstructure and mechanical properties.

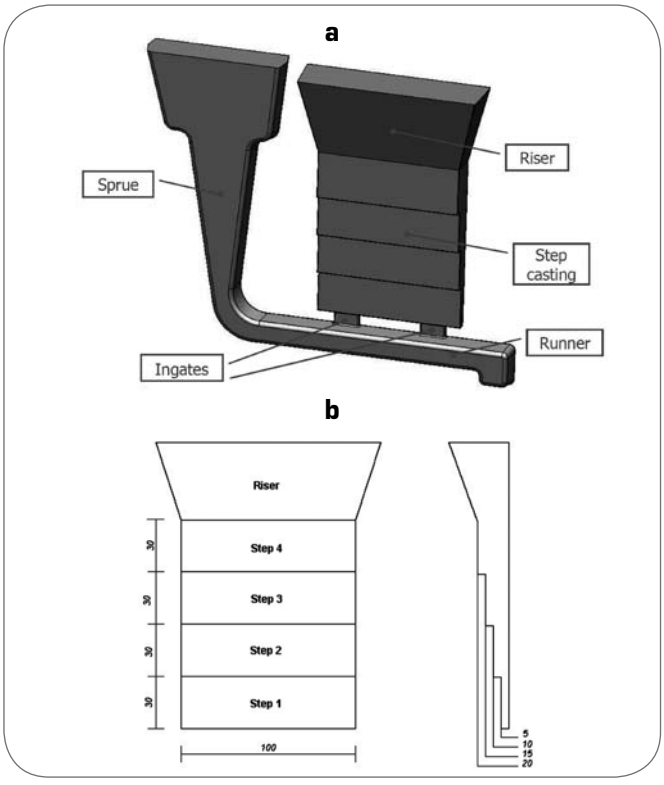

Fig. 2 ***(a) The step casting CAD geometry with (b) front and side views. All the measures are in mm.***
(a) Geometria CAD e (b) vista frontale e laterale del getto a gradini, utilizzato in questo studio. Tutte le misure sono esperesse in mm.

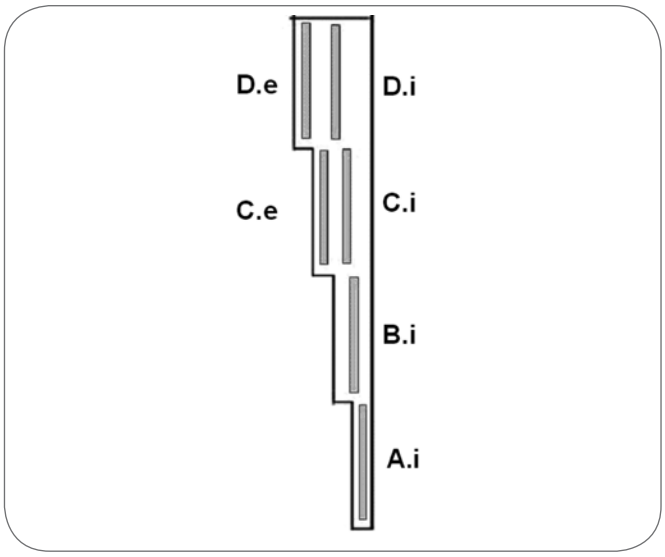

Fig. 3 ***Side view of the step casting showing sectioning scheme.***
Vista laterale del getto con evidenziate le zone di prelievo dei campioni per l'analisi microstrutturale e delle proprietà meccaniche.

Alloy	Al	Si	Cu	Fe	Mg	Mn	Ni	Ti	Zn	Others
EN-AC 46000	Bal.	8.8	3.0	0.8	0.21	0.26	0.087	0.039	0.90	0.05
EN-AC 46100	Bal.	10.8	1.8	0.8	0.13	0.18	0.089	0.046	1.29	0.05

▲ Tab. 1 ***Chemical composition of the alloys studied in the present work (wt.%).***
Composizione chimica delle leghe analizzate nel presente studio (wt.%).

The tensile specimens were 100-mm long, 20-mm wide, and 3-mm thick, with a gage length of 30 mm and a width of 10 mm, according to ASTM-B577.
The tensile tests were done on a computer controlled tensile testing machine. The crosshead speed used was 2 mm/min (strain rate~10^{-3} s^{-1}). The strain was measured using a 25-mm extensometer. At least three specimens were tested for each zone. When the experimental data differed by more than 5 pct, another tensile specimen was tested.
The samples cut from the cross section of the gage length were mechanically prepared to a 1-μm finish with diamond paste and, finally, polished with a commercial fine silica slurry for metallographic investigations. Microstructural analysis was carried out using an optical microscope and quantitatively analyzed using an image analyzer. To quantify the microstructural features, the image analysis was focused on the secondary dendrite arm spacing (SDAS), and on the size and aspect ratio of the eutectic silicon particles. Size is defined as the equivalent circle diameter (d); the aspect ratio (α) is the ratio of the maximum to the minimum Ferets. To obtain a statistical average of the distribution, a series of at least 10 photographs of each specimen were taken; each measurement included more than 1000 particles. The secondary phases, such as the Mg_2Si and $CuAl_2$ particles, and the iron-rich intermetallics were excluded from the measurements and further analysis. Average SDAS values were obtained using the linear intercept method, which involves measuring the distances between secondary dendrite arms along a line normal to the dendrite arms.

Casting simulation

The MAGMASOFT® v4.6 (2007) commercial software, with its module for gravity die casting, was used for numerically simulating the filling and solidification behaviour of analysed castings. The characteristics of the software used in this study are as follows:
- ease of physical interpretation of various steps of algorithms;
- conservation of physical properties;
- reduction of solving time.

Basic governing equations of the software are continuity equation, Navier–Stoke's equation, energy equation and volume of fluid (VoF) method for the free surface movement during the die filling. The numerical code employs the finite volume approach to convert differential equations into algebraic ones and solve them on a rectangular grid. The CAD model of the step casting was drawn and imported in the simulation software where a controlled volume mesh of 132000 cells for the die cavity was automatically generated by the software. The initial conditions for numerical simulation were defined to reproduce the casting parameters. The pouring temperature was set at 720°C, while, for the die, the temperature for the first cycle was assumed to be at a uniform temperature of 250°C. In the subsequent cycles, the initial temperature in the die is taken to be the predicted temperature distribution at the end of the previous cycle. A number of 10–15 cycles were taken after the start up to reach a quasi-steady-state temperature in the die. The thermal conductivity of the die varied in the range of 33.4–31.5 W/mK, in the working temperature range of 450–520°C. The other physical constants and properties of the die and the alloys, and their evolution with temperature, were chosen among those present in the software database, as well as the heat transfer coefficients (HTC), taking into account affecting parameters, like the type and thickness of coating, and the pouring temperature. To define the whole set of boundary conditions in the model, the process parameters (e.g. regarding the filling and cooling cycle) and the cycle time, acquired from the casting process, were imported in the software, increasing the reliability of numerical simulation. Virtual thermocouples were inserted in the different zones of the die in order to control the temperature profiles and to compare these values with the real ones. Solidification time was assessed via numerical simulation code in order to predict the final microstructure of the casting. The mechanical properties of the aluminium cast alloy were predicted by using the newly developed add-on module to the simulation software [12].

RESULTS AND DISCUSSION

In Fig. 4, typical microstructures of the step castings are reported with reference to the different step, which varies in a range of thickness between 5 to 20 mm. While Fig. 4a shows the as-cast microstructure of EN-AC 46000 alloy, in Fig. 4b the microstructure of EN-AC 46100 alloy is presented. The microstructure of the step castings analysed consists of a primary phase, α-Al solid solution, which precipitates from the liquid as the primary phase in the form of dendrites. The as-cast Al–9Si–3Cu alloy (EN-AC 46000) shows primary α-Al grains in the matrix of the eutectic structure (Fig. 4a). The eutectic structure is a mixture of the α-Al and eutectic silicon phase. The eutectic silicon can be seen in the interdendritic regions. The Al–11Si–2Cu alloy (EN-AC 46100) shows the mixed structure of the α-Al grains and eutectic (Fig. 4b). Moreover, the addition of silicon increased the fraction of the eutectic in the interdendritic region. Intermetallics compounds, such as Fe- and Cu-rich intermetallics, were also observed. A low level of microdefects, in the form of microshrinkage, was found in the specimens analysed.
The scale of microstructure in different zones of the castings was characterized by means of SDAS measurements and then correlated with mechanical properties. These data are further described. Fig. 4 presents calculated solidification times, from numerical simulation, with the corresponding microstructure within step castings of EN-AC 46000 and 46100 alloys. A general coarsening of microstructure occurs in thicker regions, quantified by SDAS values, as the result of the increased solidification time in both alloys. For every section thickness, the SDAS values were higher in the samples extracted from the inner section than the specimens from the external one.
Similar values of SDAS and solidification time for the two alloys were obtained as consequence of similar thermal properties.
Solidification times were also estimated by means of SDAS measurements using equation [13]:

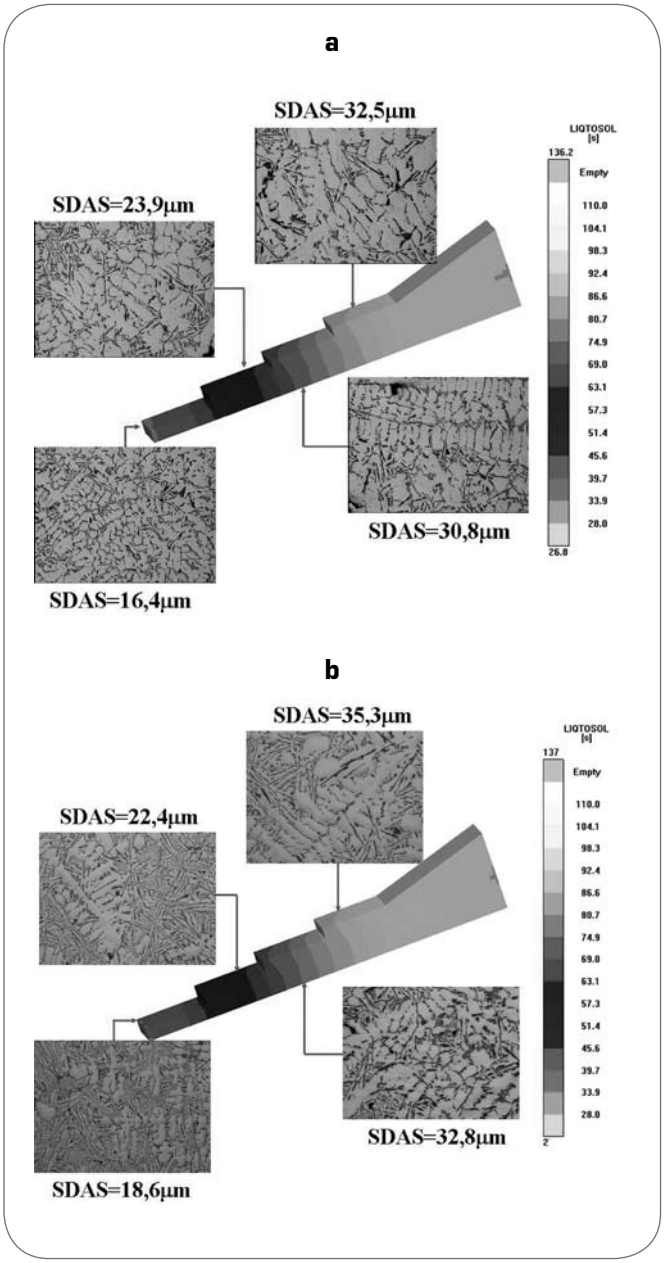

Fig. 4

Calculated solidification times with corresponding microstructure within step castings of (a) EN-AC 46000 and (b) 46100 alloys.
Valori calcolati del tempo di solidificazione per le diverse sezioni con le corrispondenti immagini microstrutturali per la lega (a) EN-AC 46000 e (b) 46100.

(2) $SDAS = 6.4\, t_s^{0.36}$

developed for aluminium casting alloys with high Si content [12]. A comparison between calculated and estimated solidification times was carried out, indicating a good relationship and testifying the ability of numerical simulation codes to predict the local solidification conditions and the characteristics of casting components.
In Tab. 2, the average values of SDAS, calculated solidification times, and size and morphology of eutectic silicon particles (i.e. equivalent diameter, d, and aspect ratio, α) are summarized.
Three-parameters lognormal distributions were fitted to eutectic Si particles diameter and aspect ratio data for the different sections of step casting. The results for EN-AC 46000 alloy are shown in Fig. 5. The coefficient of the determination R2 was used to evaluate the quality of the fitting. When R2 is equal to 1, the fit is perfect. In the present work, the coefficient R2 is 0.99, suggesting a good agreement of particle distribution with the three-parameters lognormal distribution adopted. These findings are in agreement with the results reported in Reference 8. By increasing the solidification time, i.e. the section thickness of the step, the distribution of the eutectic Si equivalent diameter becomes more spread (Fig. 5a). The equivalent diameter of eutectic Si particles with the maximum frequency shifts toward right and the absolute value of the maximum frequency decreases. In particular, this behaviour is appreciable in A.i and B.i sections.
Therefore, it can be established that by reducing the cooling rate, the microstructure is characterised by coarse eutectic Si particles, while by reducing the solidification time the formation of a high number of fine silicon particles is predominant.

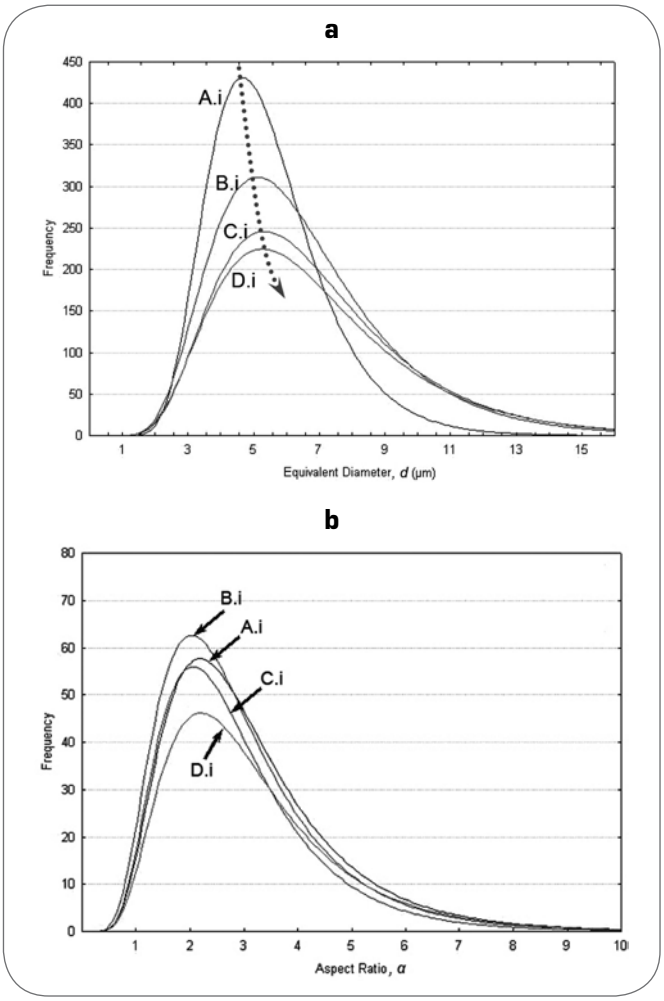

Fig. 5

Three-parameters lognormal distributions for equivalent diameter, d, and aspect ratio, α, of eutectic Si particles obtained from different sections of the step castings. Data refer to EN-AC 46000 alloy.
Distribuzione 3-parametri lognormale per i valori del diametro equivalente, d, del rapporto d'aspetto, α, delle particelle di Si eutettico, ottenuti dalle diverse sezioni del getto a gradini. I dati si riferiscono alla lega EN-AC 46000.

Alloy	Section	SDAS (μm)	Calculated solidification time (s)	Equivalent Diameter, d (μm)	Aspect Ratio, α
EN-AC 46000	A.i	16.4 (0.8)	14	5.3 (1.8)	3.0 (1.5)
	B.i	23.9 (1.8)	40	6.4 (3.0)	2.9 (1.6)
	C.e	23.5 (1.0)	38	6.4 (2.7)	2.9 (1.3)
	C.i	30.8 (0.9)	82	6.8 (3.1)	2.7 (1.4)
	D.e	25.0 (1.3)	46	7.4 (3.8)	3.0 (1.5)
	D.i	32.5 (1.9)	95	6.8 (3.3)	3.1 (1.4)
EN-AC 46100	A.i	18.6 (2.4)	20	5.5 (1.8)	4.0 (2.0)
	B.i	22.4 (1.6)	33	6.2 (2.6)	3.7 (2.0)
	C.e	26.8 (1.8)	55	6.7 (2.9)	3.6 (1.8)
	C.i	32.8 (1.3)	98	7.6 (3.8)	3.1 (1.7)
	D.e	26.9 (1.9)	56	6.7 (2.9)	4.0 (2.0)
	D.i	35.3 (2.1)	120	6.8 (3.0)	4.1 (2.3)

▲ Tab. 2

Average values of SDAS, equivalent diameter and aspect ratio of eutectic silicon particles obtained from different sections of the step castings (standard deviation in parentheses); solidification times, calculated with a numerical simulation approach, are also reported. Data refer to EN-AC 46000 and 46100 alloys.

Valori medi di SDAS, del diametro equivalente e del rapporto d'aspetto per le particelle di silicio eutettico, ottenuti dalle diverse sezioni del getto a gradini (i valori di deviazione standard in parentesi); sono inoltri riportati i valori del tempo di solidificazione per le varie zone, calcolati mediante la simulazione di processo. I dati si riferiscono alle leghe EN-AC 46000 e 46100.

Similar behaviour of the eutectic Si size was observed in the EN-AC 46100 alloy.

The impact of the solidification time on the aspect ratio of eutectic Si particles is negligible, as shown in Fig. 5b. Every step shows similar distributions of the aspect ratio of the eutectic Si particles. The irregular growth mechanism of un-modified eutectic Si particles confirms to be independent from the solidification rate, at least for the range of solidification rate investigated [14].

Generally, the distributions of the aspect ratio of the eutectic Si particles in EN-AC 46100 alloy show similar behaviour.

The correlation between solidification time and Si particles parameters is reported in Fig. 6. For both alloys, the average diameter increases significantly by increasing the solidification time from 20 to 40 seconds, while for longer times the values are steady in the range of 6.5 to 7 μm (Fig. 6a). On the other side, the aspect ratio seems to be independent from the solidification time (Fig. 6b), as previously demonstrated by means of the distribution plots in Fig. 5b.

Contrary, a relationship can be found between the aspect ratio and the Si content. If the Si amount is increased from 9 wt.% in the EN-AC 46000 alloy to 11 wt.% and EN-AC 46100 alloy, the aspect ratio of eutectic Si particles increases, indicating a more intense growing along the main axis direction of the Si particles.

In Tab. 3, the results of the mechanical investigation are shown. The values of the standard deviation confirm the presence of a low amount of microdefects, which affect the mechanical properties. However, no macrodefects were observed through the X-ray investigation.

If A.i and D.i sections are considered and compared, a reduction of 23 and 15% in UTS and 71 and 54% in elongation to fracture is observed for the EN-AC 46000 and 46100 alloys respectively, as a consequence of the different microstructure scale. In the EN-AC 46000 alloy, the UTS varies from 167 to 218 MPa and the elongation to fracture from 0.4 to 1.4%, while the change is in the range of 160 to 188 MPa for UTS and from 0.6 to 1.3% for elongation to fracture, in the EN-AC 46100 alloy. On the other hand, the solidi-

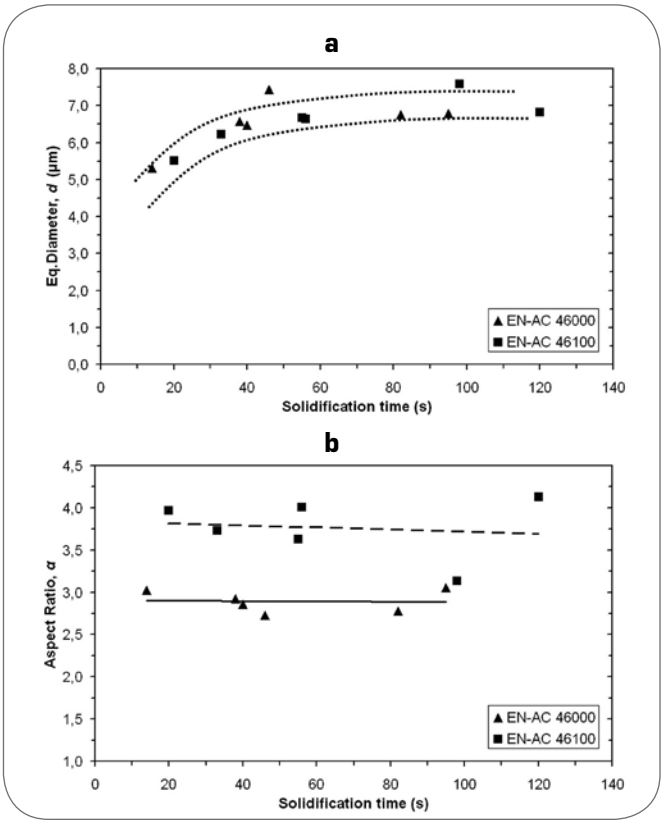

▲ Fig. 6

Variation in (a) equivalent diameter and (b) aspect ratio of eutectic silicon particles as function of solidification time.

Variazione dei valori di (a) diametro equivalente e (b) del rapporto d'aspetto delle particelle di silicio eutettico in funzione del tempo di solidificazione.

	EN-AC 46000			EN-AC 46000		
Section	YS (MPa)	UTS (MPa)	Elongation to fracture(%)	YS (MPa)	UTS (MPa)	Elongation to fracture(%)
A.i	143 (5)	143 (5)	1.4 (0.16)	120 (7)	188 (7)	1.3 (0.09)
B.i	149 (3)	149 (3)	0.8 (0.16)	132 (4)	188 (9)	1.0 (0.10)
C.e	146 (2)	146 (2)	1.1 (0.11)	131 (5)	170 (4)	0.8 (0.08)
C.i	152 (2)	152 (2)	0.7 (0.10)	129 (8)	166 (11)	0.7 (0.09)
D.e	142 (7)	142 (7)	1.0 (0.04)	119 (6)	174 (3)	1.0 (0.09)
D.i	153 (6)	153 (6)	0.4 (0.02)	122 (7)	160 (7)	0.6 (0.22)

▲ Tab. 3

Average mechanical properties obtained from different sections of the step castings (standard deviation in parentheses). Data refer to EN-AC 46000 and 46100 alloys.

Valori medi delle proprietà meccaniche ottenute per le diverse sezioni del getto a gradini (i valori di deviazione in parentesi). I dati si riferiscono alle leghe EN-AC 46000 e 46100.

fication time seems to not affect the YS of the alloys. In the EN-AC 46000 alloy, the mean YS is about 147 MPa independently from the step thickness, while the mean YS is 125 MPa in the EN-AC 46100 alloy.

In addition, the difference of the YS and UTS of the two alloys can be mainly associated to the different Cu content that improves the mechanical properties even in the as-cast temper, due to the precipitation of strengthening Al2Cu secondary phase, and to the different Si content, which decreases the ductility [15].

In order to evaluate the influence of the microstructure on the mechanical properties, the UTS and the elongation to fracture of the specimens are plotted in Fig. 7 and Fig. 8 as a function of SDAS and of the product of SDAS and aspect ratio respectively. As reported in literature [3-4], it can be observed that by increasing the SDAS values, the UTS and the elongation to fracture decrease in both alloys (Fig. 7). However, since SDAS values are similar, other microstructural parameters control the fracture mechanism of these alloys and should be taken into account to explain the existing differences in mechanical behaviour. Since the eutectic Si particles diameter is independent from the alloy type, as previously demonstrated, the aspect ratio was considered as parameter to be correlated. Fig. 8 shows the UTS and the elongation to fracture as a function of the product of SDAS and aspect ratio, showing with more evidence the different behaviour of the analysed alloys. The highest aspect ratio (~4) and Si content (~11 wt.%) in the EN-AC 46100 alloy induces probably higher tension field around eutectic Si particles, originating cracks at inferior loads [1,16].

In Figs. 9 and 10, a comparison between experimental and simulated values in terms of mechanical properties of EN-AC 46000 and 46100 alloys is shown.

In the EN-AC 46000 step castings, the YS shows a difference of about 15% between experimental and simulated values (Fig. 9a). While an average forecast values of 130 MPa is provided by the simulation code, the experimental YS is about 149 MPa, i.e. the numerical simulation underestimates the YS values. The difference between experimental and simulated values is reduced considering the UTS and the elongation to fracture. In general, the UTS values in D.i and C.i sections differ of about 4%, while in the remaining sections the simulated values are about 13% lower than the experimental ones (Fig. 9b). As it is possible to observe the relationship is good for the elongation to fracture (Fig. 9c).

If the EN-AC 46100 step castings are considered, it was demonstrated that the experimental and simulated values are similar: the YS, UTS and elongation to fracture differ up to 5% (Fig. 10).

It can be suggested that numerical simulation is an useful tool in the design stage, allowing the optimization of the geometry of casting components, dies and process parameters, thereby, making the design and development process more time and cost efficient. It should be mentioned that this simulation tool is still under development and comprises only a restricted range of alloying elements [12].

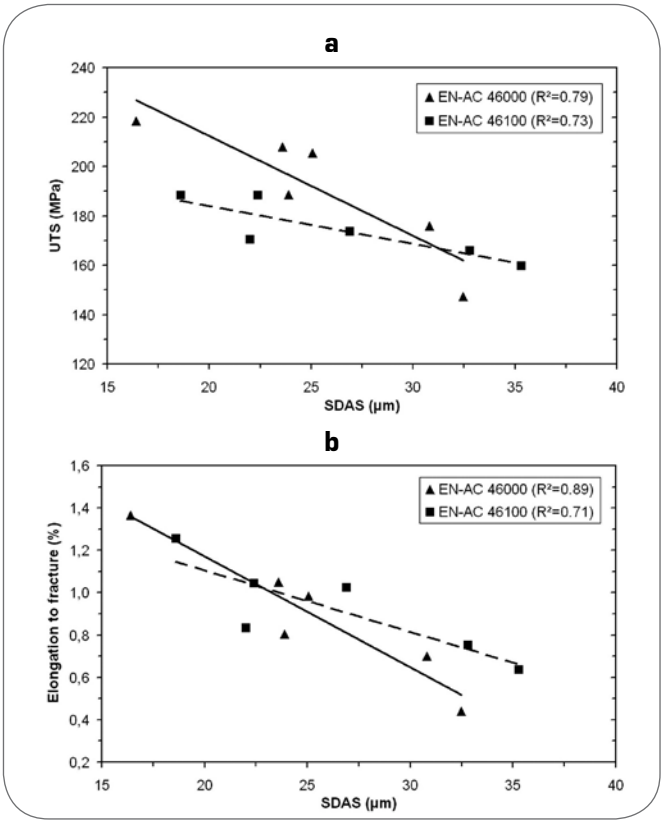

▲ Fig. 7

Average (a) UTS and (b) elongation to fracture as a function of SDAS; coefficient of determination, R2, are given. Data refer to EN-AC 46000 and 46100 alloys.

Valori medi di (a) UTS e (b) allungamento a rottura in funzione dello SDAS. E' inoltre riportato in coefficiente di determinazione, R2. I dati si riferiscono alle leghe EN-AC 46000 e 46100.

CONCLUSIONS

The effects of microstructural parameters such as SDAS, size and morphology of eutectic silicon particles on mechanical properties of EN-AC 46000 and 46100 alloys have been investigated. In addition, the validation of the results provided by a numerical simulation approach has been performed. Based on the results obtained in the present study, the following conclusions can be drawn.

- The equivalent diameter and the aspect ratio of eutectic Si particles follow three-parameter lognormal distributions.
- While the distribution of the equivalent diameter depends on solidification time, the distribution of the aspect ratio is less sensible, indicating the irregular growing mechanism of un-modified eutectic silicon.
- The average size of eutectic silicon particles is similar in both EN-AC 46000 and 46100 alloys, while the aspect ratio of EN-AC 46100 is higher, probably due to higher Si content.
- The mechanical properties, i.e. the UTS and elongation to fracture, depend on SDAS and on the aspect ratio of the eutectic Si particles, which seems an alloy-related parameters. Increasing the SDAS and the aspect ratio values, the UTS and the elongation to fracture decrease.
- The difference in the mechanical properties of the two alloys is the consequence of different chemical composition. Higher Cu and Mg contents in the EN-AC 46000 alloy allows to increase the YS, while a lower Si amount permits to enhance the ductility, reaching higher UTS and elongation to fracture values than the EN-AC 46100 alloy.
- Since numerical simulation results reproduce the experimental data with a good accuracy, it can be stated that numerical simulation is a useful tool for the reduction of time and costs in the design stage.
- The present investigation has been carried out on un-modified gravity cast alloys; in the case of higher cooling rate, modification or heat treatment, attention should be also paid to the size of eutectic Si particle, as a parameter affecting the mechanical behaviour.

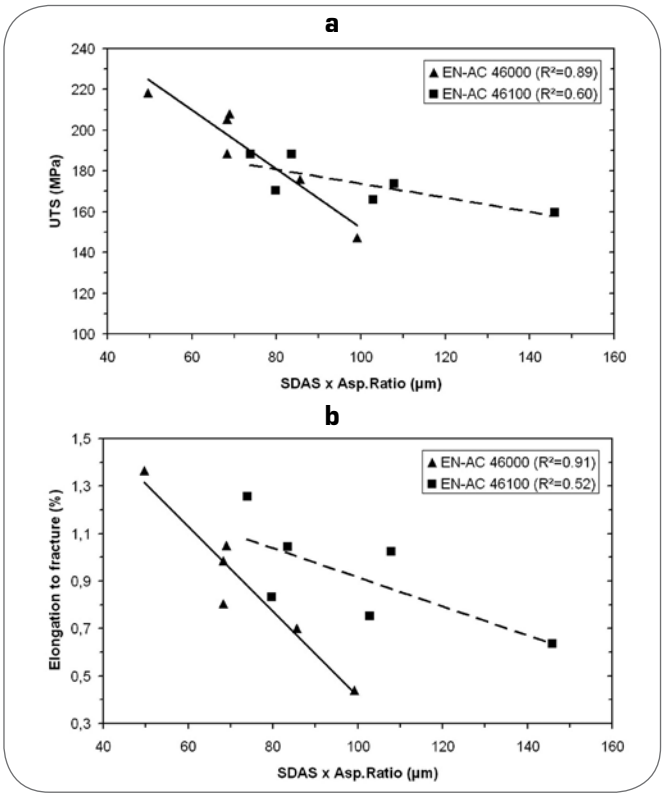

Fig. 8

Average (a) UTS and (b) elongation to fracture as a function of the combined parameter SDAS x Aspect ratio; coefficient of determination, R2, are given. Data refer to EN-AC 46000 and 46100 alloys.

Valori medi di (a) UTS e (b) allungamento a rottura in funzione del prodotto tra SDAS e rapporto d'aspetto. E' inoltre riportato in coefficiente di determinazione, R2. I dati si riferiscono alle leghe EN-AC 46000 e EN-AC 46100.

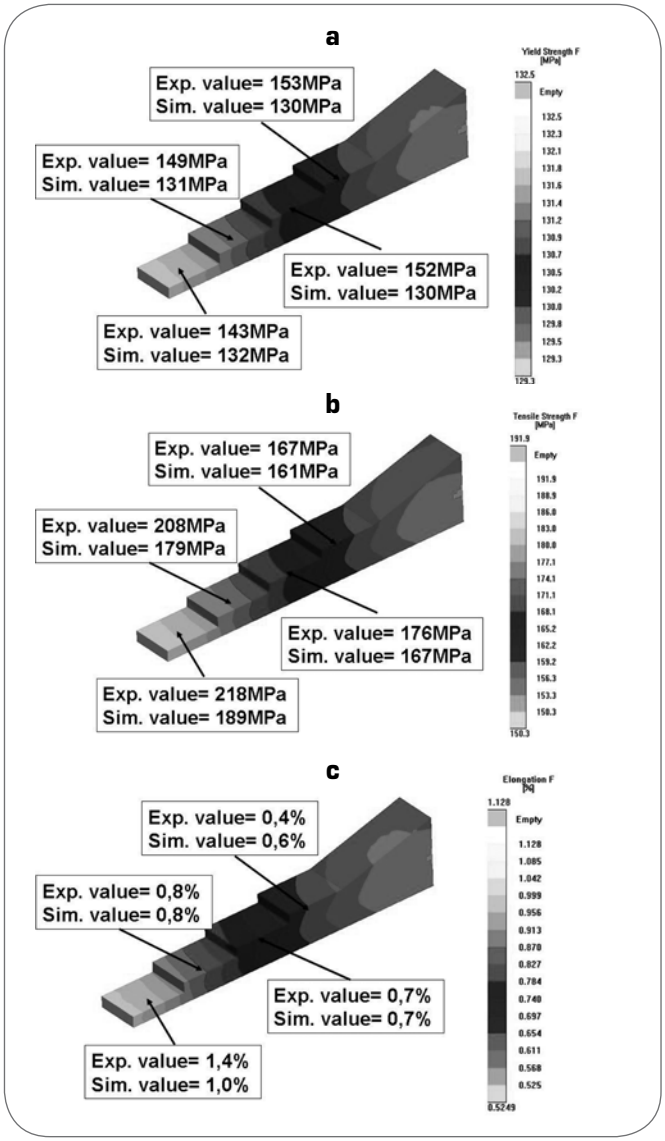

Fig. 9

Comparison between experimental and simulated mechanical properties in EN-AC 46000 step casting. The images refer to (a) YS, (b) UTS and (c) elongation to fracture.

Confronto tra i valori delle proprietà meccaniche ottenuti sperimentalmente e mediante simulazione di processo per il getto colato con lega EN-AC 46000. Le immagini si riferiscono a (a) YS, (b) UTS e (c) allungamento a rottura.

ACKNOWLEDGMENTS

The European Project NADIA- New Automotive components Designed for and manufactured by Intelligent processing of light

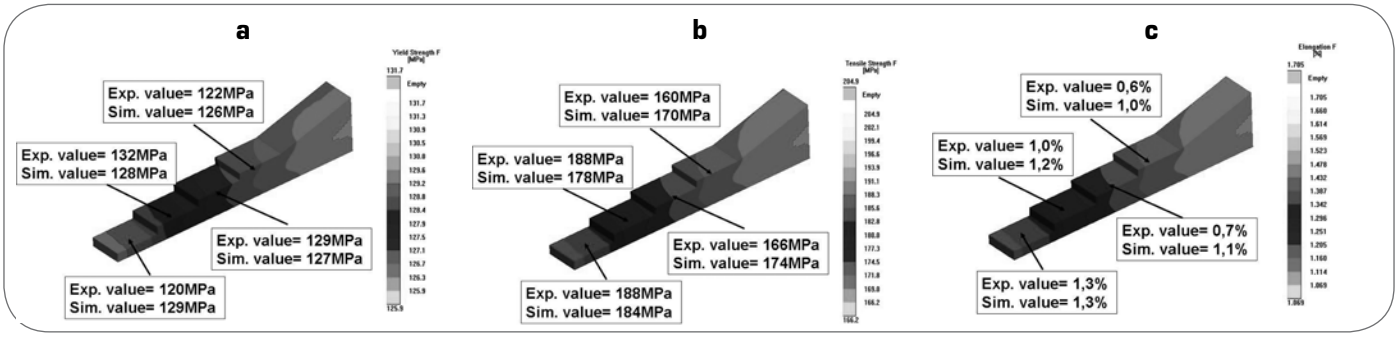

Fig. 10

Comparison between experimental and simulated mechanical properties in EN-AC 46100 step casting. The images refer to (a) YS, (b) UTS and (c) elongation to fracture.

Confronto tra i valori delle proprietà meccaniche ottenuti sperimentalmente e mediante simulazione di processo per il getto colato con lega EN-AC 46100. Le immagini si riferiscono a (a) YS, (b) UTS e (c) allungamento a rottura.

Alloys (NMP-2004-SME 3.4.4.5, contract n.026563-2) is gratefully acknowledged for financial support. Many thanks are due to dr. R. Molina (Teksid Aluminum), dr. G.F. Capra and dr. L. Capra (Raffineria Metalli Capra), and dr. G. Valente (DTG) for their contribution to the experimental work.

REFERENCES

1] S.G. SHABESTARY, F. SHAHRI, J. Mater. Sci. 39, (2004), pp.2023-2032
2] S. VISWANATHAN, A.J. DUNCAN, A.S. SABAU, Q. HAN, W.D. PORTER, B.W. RIEMER, AFS Trans. 106, (1998), pp.411-417.
3] V. RONTÓ and A. ROÓSZ, Int. J. Cast Metals Res. 13, (2001), pp.337-342.
4] F. BONOLLO, G. TIMELLI, N. GRAMEGNA, B. MOLINAS, Proc. 3rd Int. Conf. High Tech Die Casting, Vicenza (2006), AIM, Milano, paper 67.
5] F. BONOLLO, G. TIMELLI, G. MAZZACAVALLO, R. MOLINA, Proc. 30th Convegno Nazionale AIM, Vicenza (2004), AIM, Milano, paper 137.
6] S.T. McCLAIN, J.T. BERRY and B. DAWSEY, AFS Trans. 111, (2003), pp.147-158.
7] G. TIMELLI, F. BONOLLO, Proc. Int. Conf. Aluminium Two Thousand, Florence (2007), Interall, Modena.
8] M. TIRYAKIOGLU, Mater. Sci. Eng. A 473, (2008), pp.1-6.
9] C.H. CÁCERES, J.R. GRIFFITHS, Acta Mater. 44, (1996), pp.25-33
10] Q.G. WANG, C.H. CÁCERES, Mater. Sci. Eng. A 241, (1998), pp.72-82.
11] FOSECO, Dycote® Manual – Coatings for non-ferrous metal die-casting, pp.1-28.
12] S. SEIFEDDINE, M. WESSEN, I.L. SVESSON, Metall. Sci. Tech. 24, (2006), pp. 26-32.
13] 1L.BACKERUD, G.CHAI, J.TAMMINEN, Solidification Characteristic of Aluminum Alloys-Vol.2: Foundry Alloys. American Foundrymen's Society, Inc., IL, USA(1990).
14] W. KURZ and D.J. FISHER, Fundamentals of solidification, Cap.5. Trans. Tech. Publications, Switzerland (1998).
15] C.H. CACERES, I.L. SVENSSON, J.A. TAYLOR, Int. J. Cast Metals Res., 2003,15, 531-543
16] Q.G. WANG, C.H. CACERES, J.R. GRIFFITHS, Metall. Mater. Trans. A, December 2003, 2901-2912

ABSTRACT

CORRELAZIONE TRA MICROSTRUTTURA E CARATTERISTICHE MECCANICHE IN LEGHE Al-Si DA FONDERIA

Parole chiave: alluminio e leghe, solidificazione, fonderia, metallografia, simulazione numerica

Nel presente lavoro è stata analizzata l'influenza della microstruttura e dei parametri di processo sul comportamento meccanico di leghe Al-Si da fonderia. Due le leghe considerate: la lega EN-AC 46000 e la lega EN-AC 46100, che differiscono principalmente per il contenuto di Si e Cu; esse sono state colate in uno stampo permanente ottenendo un getto a gradini con uno spessore variabile tra i 5 e i 20 mm (Fig.2). I campioni, ricavati sezionando i getti considerati, sono stati quindi esaminati utilizzando tecniche di analisi metallografica e d'immagine che hanno permesso una valutazione quantitativa dei parametri microstrutturali relativi alla fase α-Al e alle particelle di Si eutettico.

I risultati ottenuti hanno mostrato l'influenza della velocità di solidificazione sui valori di SDAS e delle dimensioni delle particelle di Si eutettico. In particolare, all'aumentare dello spessore del getto e, quindi, al diminuire della velocità di solidificazione, si è ottenuta una microstruttura via via più grossolana caratterizzata da valori crescenti di SDAS e di diametro equivalente delle particelle di Si (Figg.4-6). Viceversa il rapporto d'aspetto di tali particelle non sembra essere influenzato dal tempo di solidificazione ma, piuttosto, dal contenuto di Si; passando da circa il 9% all11% di Silicio il valore medio del rapporto d'aspetto aumenta da ~3 a ~4.

I valori microstrutturali sono stati quindi correlati alle proprietà meccaniche dei getti considerati. Si è notato come all'aumentare dello SDAS e del rapporto d'aspetto delle particelle di Si, i valori di UTS e di allungamento a rottura diminuiscano (Figg.7-8). Tale diminuzione è stata più evidente per la lega EN-AC 46100 in virtù di un valore medio del rapporto d'aspetto più elevato che produce una tensione maggiore attorno alle particelle di Si, favorendone la rottura.

Infine, le proprietà meccaniche ottenute sperimentalmente sono state confrontate con quelle fornite da un software di simulazione. I risultati forniti dal codice di calcolo hanno mostrato una buona attendibilità, discostandosi all'interno di un intervallo accettabile dai valori reali misurati nel getto(Figg.9-10). La simulazione di processo si pone quindi come un utile strumento nella fase di progettazione per ridurre tempi e costi ad essa associati.